Korean J. Chem. Eng., 34(1), 225-230 (2017)
DOI: 10.1007/s11814-016-0264-6

pISSN: 0256-1115
eISSN: 1975-7220

Synthesis of aragonite-precipitated calcium carbonate from oyster shell waste via a carbonation process and its applications

Chilakala Ramakrishna*, Thriveni Thenepalli, Choon Han***, and Ji-Whan Ahn**,†**

*Department of R&D Team, Hanil Cement Corporation,
302 Maepo-ri, Maepo-eup, Danyang-gun, Chungcheongbuk-do 27003, Korea
**Mineral Processing Division, Korea Institute of Geoscience and Mineral Resources (KIGAM), Daejeon 34132, Korea
***Chemical Engineering Department, Kwangwoon University, Nowon-gu, Seoul 01899, Korea
(*Received 31 March 2016 • accepted 10 September 2016*)

Abstract−Oyster shells are abundantly available in nature without eminent use and are dumped into landfills in vast quantities. Their improper disposal causes environmental problems, resulting in a waste of natural resources. Recycling shell waste could potentially eliminate the environmental problems and, moreover, convert the waste into high-value-added products, such as synthetic precipitated calcium carbonate (PCC), which can be obtained from oyster waste and which is used to enhance the mechanical properties of various materials. It can also be used as a filler material in the plastic and paper industries. This study presents a simple method for the extraction of aragonite needles from oyster shell waste via a carbonation process. The obtained aragonite-precipitated calcium carbonate (PCC) is characterized by XRD and SEM, which is used to assess the morphology and particle size. Using the proposed process, oyster shell waste powder was calcined at 1,000 °C for 2 h, after which the calcined shell powder was dissolved in water for hydration. The hydrated solution was mixed with an aqueous solution of magnesium chloride at 80 °C and CO_2 was then bubbled into the suspension for 3 h to produce needle-shaped aragonite PCC. Finally, aragonite-type precipitated calcium carbonate was synthesized from the oyster shell powder via a simple carbonation process, yielding a product with an average particle size of 30-40 μm.

Keywords: Oyster Shell Waste, Calcium Carbonate, Aragonite PCC, Mineral Filler

INTRODUCTION

In developing economies across the Pacific region, aquaculture has become the fastest growing industry for producing animal protein [1], and global aquaculture production expanded at an average annual growth rate of 6.2% from 2000-2012 (compared to only 10% from 1980-1990). For the decade 2012–2022, aquaculture is forecasted to grow between 29 and 50% [2]. China is the largest mollusk producer, accounting for approximately 83.4% of worldwide production. Table 1 shows mollusk production by country (shell tons) for the year 2013 [3]. This intensive production, however, generates a large amount of shell waste, estimated at an average of 270,000 tons/year [4], and more than 70% of shell waste is dumped into natural waters and landfills, causing strong and unpleasant odors as a result of the decomposition of fresh muscles attached to oysters [5].

On the southern coast of South Korea, oyster shell waste is dumped into coastal areas as a by-product of the marine aquaculture industry. A large amount of oyster shell waste is generated in landfill sites, which creates problems for fishermen in terms of collection, securing of landfill sites, and the transport of oyster shells [6]. In addition, oyster shell waste causes many environmental problems, including public water pollution, damage to the natural landscape, and health/sanitation problems.

Table 1. Mollusks culture production (with shell, tons) by country (Source: Adapted from reference - 3)

Producer	Molluscs (Tones)	Percentage (%)
China	12728046	83.4
Japan	332460	2.2
Republic of Korea	291024	1.9
Chile	252528	1.7
Thailand	217467	1.4
Viet Nam	179163	1.2
Spain	164976	1.1
United states of america	160458	1.1
France	156980	1.0
Italy	110645	0.7
Others	**668875**	**4.4**
World	**15262622**	**100**

Specific problems caused by oyster shell waste include increased amounts of shell waste, the pollution of marine ecosystems due to landfill spillover, offensive odors due to negligence, increased costs and expenses incurred due to necessary treatments of oyster shell waste, and less demand for recycled materials (e.g., filler, fertilizer) from oyster shells. Oyster shell waste has become a serious prob-

†To whom correspondence should be addressed.
E-mail: ahnjw@kigam.re.kr

lem, and in most cases, the shell waste is disposed of or dumped in fields and/or public water sources. Waste left to sit for a long time can create noxious odors as a consequence of the decay of the remaining attached muscles or the decomposition of salts into gases such as H_2S, NH_3, and amines.

Approximately 30% to 50% of collected oysters are actually utilized, with the remaining shell waste discarded [7]. Thus, the recycling of oyster shell waste is an emerging issue for the mariculture industry. The utilization of oyster shells as a sorbent for incineration and desulfurization processes is potentially very useful in marine ecosystems, preventing damage to the natural landscape and mitigating sanitation/health problems [8]. Environmental engineering research has been conducted in China and Japan on oyster shell waste recycling processes, but research on oyster shell waste in relation to water purification processes remains limited [4].

Oyster shells are not simply aquatic waste material but are potentially a valuable resource for new industries. Oyster shells are used as a construction material and as sludge conditioners, eutrophication control materials, soil conditioners and fertilizers [9-11]. The main component of oyster shell powder is $CaCO_3$, which is converted to CaO by heat treatment. It exhibits antibacterial activity [12] and effectively kills some of the most pathogenic viruses, such as *Escherichia coli* O-157:H7 [13].

The recycling of oyster shell waste is a viable alternative to its normal disposal. De-Alvarenga et al. [14] conducted a life cycle assessment (LCA) for oyster waste in southern Brazil. To reduce the amount of shell waste, major resources have been spent on developing possible applications. However, until recently, the use of oyster shells has been limited to calcium supplements and soil conditioners. Long-term effort is needed to develop potential recycling processes for oyster shell waste to reduce environmental problems.

The major component of oyster shells is calcium carbonate, which has a structure composed of three layers: an outer layer made of chitin, an inner layer consisting of both calcite and aragonite, and an interbedded layer with protein molecules. The average composition of the minerals in the shell is approximately 90% calcite and 10% aragonite [15]. Fig. 1 shows the total content of $CaCO_3$ (wt% of a dry sample) present in limestone and oyster shells and the relative abundance of both calcite and aragonite.

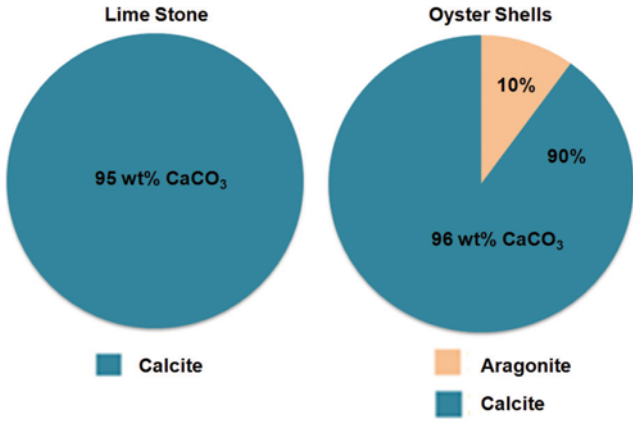

Fig. 1. Mineralogical composition of limestone and oyster shells total content of $CaCO_3$ and the relative abundance of calcite and aragonite (Source: Adapted from reference 15).

Precipitated calcium carbonate ($CaCO_3$) is the most widely used inorganic filler for polymers [16]. Oyster shell waste consists mainly of $CaCO_3$ (approximately 95%) with a small amount of bio-macromolecules, such as proteins, glycoproteins and polysaccharides [17,18], and may be feasible as a commercial filler for polymers with unique mechanical properties [19]. Recycled shells are widely utilized as a filler material in the polymer industry. Corni et al. [20] reported that nacre from Pinctada shells has high tensile strength (140-170 MPa) and a high Young's modulus (60-70 GPa), implying its usefulness for improving the mechanical properties of polymers. Chong et al. [21] prepared composite materials with recycled polyethylene and oyster shell powder for enhanced mechanical properties compared to those of neat polyethylene. Lin et al. [22] prepared scallop shell/polypropylene (PP) composites; their results indicated that the incorporation of shell powder greatly increased the impact strength of PP. However, it was also found that an excessive addition of $CaCO_3$ could decrease the impact properties of PP [23].

Li et al. [24] reported higher elongation at the break point as well as good tensile strength, yield strength and yield strain of polypropylene composites filled with bio-aragonite compared with commercial $CaCO_3$. Additionally, de-Melo et al. [25] found that the incorporation of mollusk shell waste with high-density polyethylene could increase the degree of crystallinity and stiffness. Recycling shell waste offers many advantages in various fields. However, natural limestone with purity levels exceeding 90 wt% of $CaCO_3$ is usually used in waste water treatment processes. Similarly, oyster shells consist of 90 to 95 wt% $CaCO_3$, making this material an excellent alkalinity source for waste water treatment purposes.

Our main objective was to synthesize needle-shaped aragonite-precipitated calcium carbonate (PCC) from oyster shell waste via a simple carbonation process. The PCC can then be utilized as a filler material for improving the mechanical properties of products in the plastics and paper industries.

EXPERIMENTAL PROCEDURE FOR ARAGONITE SYNTHESIS FROM OYSTER SHELL WASTE VIA A CARBONATION METHOD

The starting materials were $MgCl_2$ of 95% purity (Junsei Company, Japan), oyster shell waste (Namhae, South Korea), and pure CO_2 gas (Jeil Gas Company, South Korea).

We used oyster shell waste collected from waterfront areas in Namhae, South Korea, and cleaned with alcohol and water to remove impurities attached to the surfaces. The cleaned and dried oyster shells were milled using comminution equipment until a fine powder was obtained with a particle size of less than 100 μm. This fine oyster shell powder was calcined in an electric furnace at a constant temperature of 1,000 °C for 2 h, which was increased to this point at a rate of 10 °C/min.

The calcined raw materials were mechanically ground for 1 h until the particle size was less than 70 μm. The fine powder was processed to hydration (40 g/lit) with distilled water at 80 °C for 1 h and filtered with a 200 mesh. The filtrate was collected and washed three times with distilled water and filtered again with a 325 mesh and dried at 80 °C for 12 h.

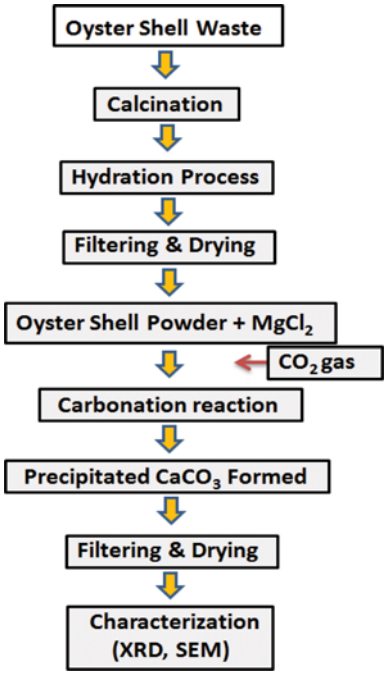

Fig. 2. Calcium carbonate synthesized by carbonation process.

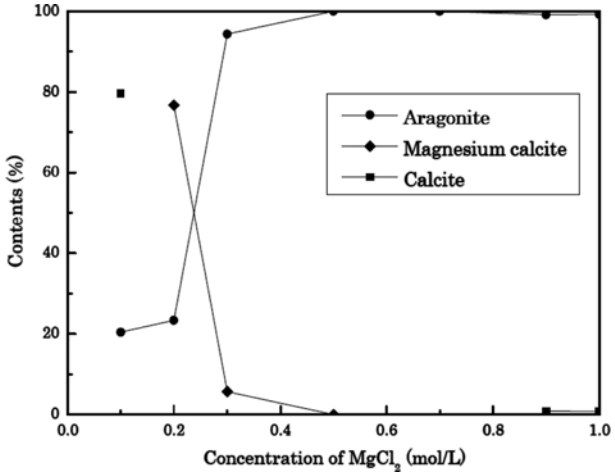

Fig. 3. Changing the formation yield of products with the addition of 0.6 M $MgCl_2$.

After the hydration and filtering process, we obtained 25 g of a dried Ca^{2+}-rich oyster shell fine powder, which was then used as a Ca^{2+} source for the carbonation process to synthesize calcium carbonate. During this process, 25 g/lit of the dried calcium-rich oyster shell powder was added to 0.6 M of a magnesium chloride solution, and gaseous carbon dioxide (CO_2) was injected into the $MgCl_2$-Ca^{2+}-rich oyster powder suspension at pH 8-10 for a 3 h carbonation reaction to form a calcium carbonate precipitation, as shown in Fig. 2. The carbonation reaction began with the hydration of carbon dioxide and the ionization of calcium hydroxide. The calcium and carbonate ions reacted together to form a calcium carbonate precipitate. The effects of the carbonation temperature, reaction time, and carbon dioxide flow rate on the morphology of the resulting product were investigated.

RESULTS AND DISCUSSION

During this carbonation process, the $MgCl_2$ concentration, temperature, reaction time, and carbon dioxide flow rates play a key role in the synthesis of aragonite calcium carbonate.

1. $MgCl_2$ Effect on the Formation of Aragonite via the Carbonation Process

Aragonite crystal can be prepared from solutions containing calcium (Ca^{2+}) and carbonate (CO_3^{2-}) ions through the carbonation process. During this carbonation reaction, the formation yield of aragonite is significantly increased with an increase in the amount of $MgCl_2$, up to a concentration of 0.6 M. The presence of magnesium (Mg^{2+}) ions is most effective for the formation of aragonite, and it suppresses calcite nucleation as well as the growth of calcite crystals. Fig. 3 shows the total yield of the product formation with an addition of 0.6 M $MgCl_2$ [26].

However, when the $MgCl_2$ solution was added with a high concentration, Mg^{2+} ions were ionized from the solution as the reaction time increased. During the aragonite synthesis process, many Mg^{2+} ions became incorporated into the Ca^{2+} ion sites of the calcite lattice, leading to the production of Mg-calcite. Calcite and Mg-calcite structures have similar hexagonal shapes, but Ca^{2+} (0.99 A°) and Mg^{2+} (0.66 A°) have an ionic radius difference of (0.33 A°). The concentration of Mg^{2+} ions increased in the reaction mixture solution, with many more of the smaller Mg^{2+} ions displaced by the larger Ca^{2+} ions from calcite, becoming incorporated into the Mg-calcite lattice. As a result, the concentration of the Mg^{2+} ions increased, and the Mg-calcite also increased, which led to the availability of Ca^{2+} ions at a high concentration for the synthesis of aragonite needles, and, consequently, an increase in the yield of aragonite [27].

2. Effect of the Temperature

Temperature is one of the key determining factors in the formation of aragonite. The first experimental measurement of this temperature coefficient was found on the basis of the inorganic precipitation of aragonite or an aragonite-calcite mixture from seawater in a temperature range of 0 °C to 80 °C [28]. The phase transition of aragonite to calcite in marine shells and coral occurs at a lower temperature [29]. Some results show that aragonite is synthesized at room temperatures when the Kitano method is applied from a supersaturated solution of calcium bicarbonate in the presence of additives or self-assembled monolayers [30], with this even achieved at slightly elevated temperatures in other work [31]. Uniform needle-shaped aragonite particles with a mean length of 45 μm and an aspect ratio of roughly 10 were obtained at 3 h of aging in a mixed solution containing 0.25 mol $CaCl_2$ and 0.75 mol urea at 90 °C by a homogeneous precipitation process without an adjustment of the pH [32]. Many researchers have investigated the dependency of the temperature on the formation of aragonite PCC and aragonite whiskers [33-35].

The aragonite form of $CaCO_3$ is a thermodynamically metastable crystalline structure that can easily transform into a calcite phase in an aqueous solution. However, the present work reveals needle-like aragonite synthesis when gaseous CO_2 is injected into an aqueous

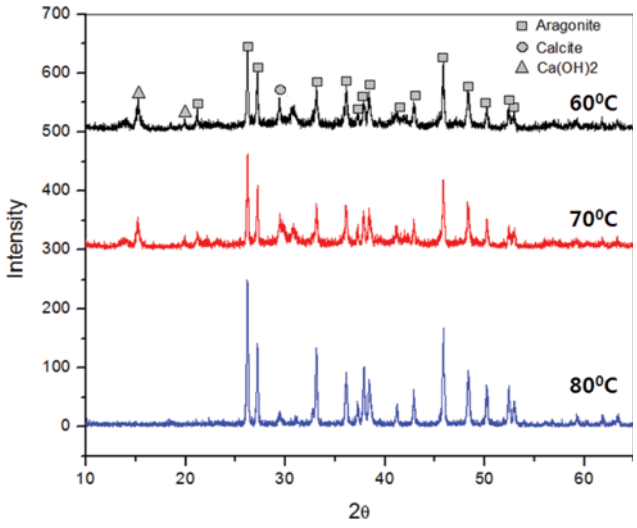

Fig. 4. XRD analysis of needle shape aragonite synthesis from oyster shell waste by carbonation process at different temperatures.

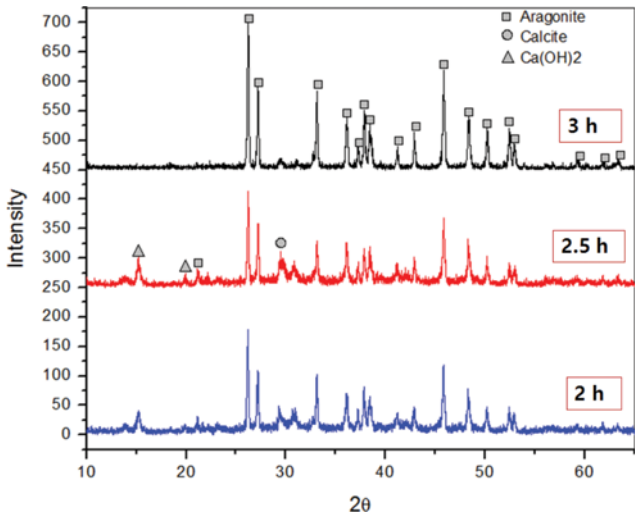

Fig. 6. XRD analysis of aragonite needle at different carbonation time durations.

mixture solution of oyster shell powder and an $MgCl_2$ solution at different temperatures (60, 70 and 80 °C). The formation of aragonite is increased with an increase in the temperature to 80 °C by the carbonation process, and the formation of needle-like aragonite at 80 °C with 50 cc carbon dioxide flow rates is clearly observed via an XRD analysis, as shown in Fig. 4. In addition, Fig. 5 shows the morphology of the aragonite needles according to scanning electron microscopy results.

3. Effect of the Reaction Time

Many reports have analyzed different time effects on the carbonation process. Ge et al. [36] reported that at a carbonization time of 0.5 h, calcite and vaterite were synthesized. When the carbonization time was extended to 1-1.5 h, the calcite phase was transformed into aragonite and vaterite. However, when the carbonization time was extended to 2 h, pure aragonite was synthesized, and the aragonite content gradually increased. Additionally, the vaterite content initially increased and then decreased. Similarly, the calcite content also decreased with an increase in the carbonization time. After a carbonization time of 4 h, the aragonite content was 81.35%, the calcite level was 4.56%, and vaterite was found at a rate of 14.09% indicating that increasing the carbonization time to 4 h is most helpful for the formation of aragonite.

We analyzed different time effects on the carbonation process. In this process, we observed needle-like aragonite synthesis when gaseous CO_2 was injected into an aqueous mixture solution of oyster shell powder and an $MgCl_2$ solution at different time durations (2, 2.5 and 3 h) at a constant temperature. The aragonite needles obtained after a reaction time of 3 h by the carbonation process were confirmed in the XRD results (Fig. 6), and aragonite needle morphology shown in Fig. 7 was confirmed in scanning electron microscopy (SEM) images.

4. Effect of the Carbon Dioxide (CO_2) Flow Rate

The carbonation process was in an aqueous medium, and different CO_2 gas flow rates between 40 mL/min to 100 mL/min at 80 °C were assessed. However, after a certain limit, the higher flow rate no longer had any effect. The main reason, CO_2 molecules mobility was higher in the water [37]. The CO_2 gas flow rate (50 mL/min) was suitable for embedding with unreacted calcium hydroxide crystals and other calcium carbonate polymorphic phases that appeared. This can be clearly observed from the XRD analysis at different CO_2 flow rates, as presented in Fig. 8 and Fig. 9, which show scanning electron microscopy (SEM) images of the needle-shaped aragonite calcium carbonate created with different CO_2 flow rates.

5. Effect of the Aragonite PCC Yield Obtained via the Carbonation Process with Different Times, Temperatures and CO_2 Flow Rates

The total obtained aragonite yield by the carbonation process

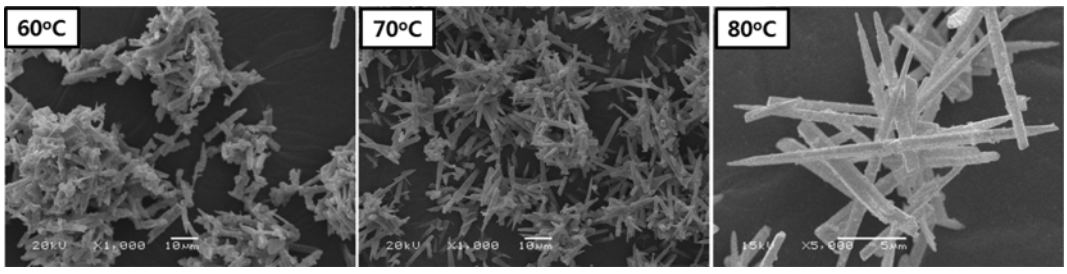

Fig. 5. Effect of different carbonation temperatures on the morphology of aragonite needles, determined by scanning electron microscopy.

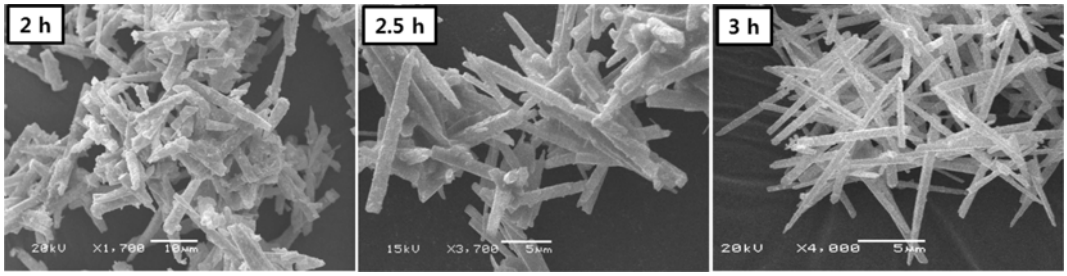

Fig. 7. Effect of different carbonation time durations on the morphology of aragonite needles, determined by scanning electron microscopy.

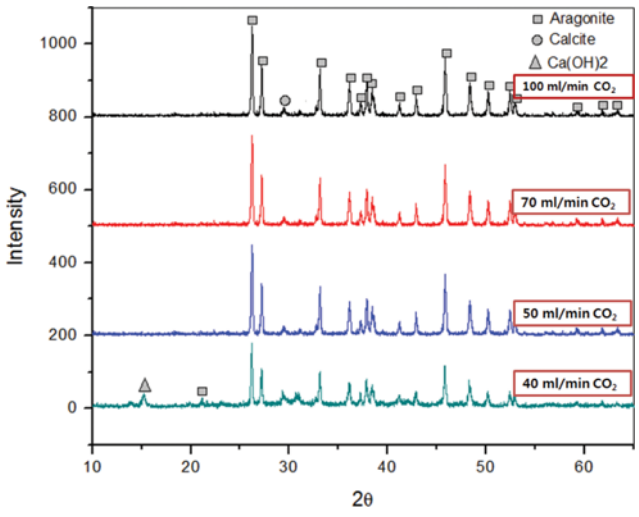

Fig. 8. XRD analysis of aragonite needles at different CO_2 flow rates.

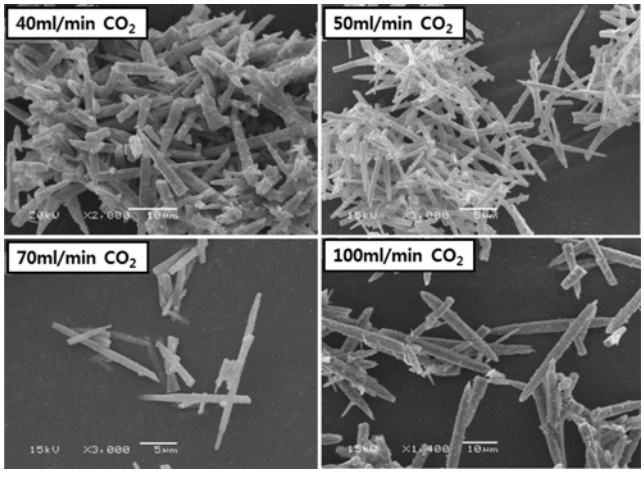

Fig. 9. Effect of different CO_2 flow rates on the morphology of aragonite needles by scanning electron microscopy.

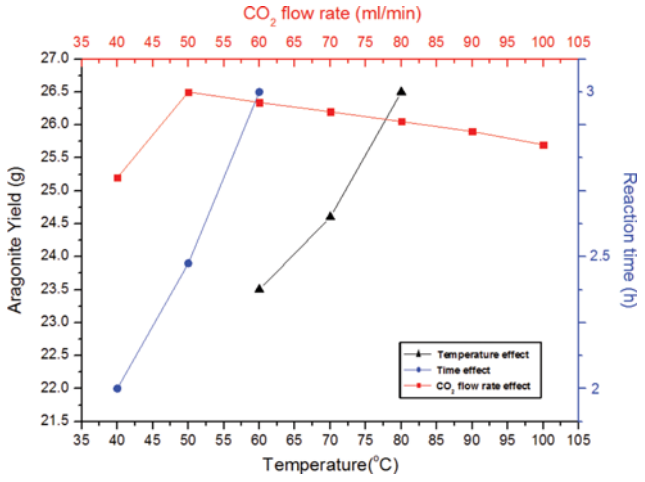

Fig. 10. Aragonite yield weight (g) changes with different temperatures, time and CO_2 flow rates.

mainly depends on the temperature, reaction time and CO_2 flow rate. In this process, we used 40 g of calcined oyster shell powder processed via hydration, filtering and drying, as described in the experimental procedure. From this, we obtained 25 g of purified calcium-rich dried oyster shell powder, which was used as a Ca^{2+} source for carbonation to synthesize aragonite.

After the carbonation process, the needle-like aragonite yield increased gradually (23.5, 24.6 and 26.5 g) with an increase in the temperature (60, 70 and 80 °C) at a carbon dioxide flow rate of 50 mL/min for a 3 h reaction. Similarly, the reaction time also affects the aragonite yield; hence, the carbonation reaction time duration was increased gradually (2, 2.5 and 3 h) at 80 °C, and, simultaneously, the synthesis of aragonite also increased (22, 23.8 and 26.5 g).

Carbon dioxide (CO_2) also plays a key role in the formation of aragonite; thus, the CO_2 flow rate was increased from 40 mL/min to 100 mL/min gradually for a 3 h reaction time at 80 °C. A high amount (26.5 g) of aragonite was synthesized at a CO_2 flow rate of 50 mL/min. The aragonite yield was slightly decreased with an increase in the CO_2 flow rate to 100 mL/min by the carbonation process. These results indicate that a low carbon dioxide flow rate is most suitable for aragonite synthesis. Fig. 10 clearly indicates that the aragonite yield changes after the carbonation process with different experimental parameters.

CONCLUSION

Needle-like aragonite was synthesized from oyster shell waste by a simple carbonation procedure. Aragonite needles with a width of 3 μm and a length of 40 μm were formed by feeding 50 mL/min of CO_2 gas into 25 g of a calcium-rich solution from oyster shell powder with 0.6 M $MgCl_2$ at 80 °C for 3 h (a carbonation process without any additives). The morphology of $CaCO_3$ is sensitive to the $MgCl_2$ concentration, carbonation time, CO_2 flow rate, and

carbonation temperature. Increasing the Mg^{2+} concentration, reaction time and temperature for the carbonation process promotes the formation of $CaCO_3$ with a needle-like morphology. However, oyster shell waste is reused as substitute material, and its effect must be evaluated as it contains a high amount of $CaCO_3$ and fewer organic matrices; hence, it is better to use it directly instead of limestone for the synthesis of needle-shaped aragonite by a carbonation process. These results demonstrate that needle-shaped aragonite crystals synthesized from oyster shell waste under optimized conditions have a strong potential for use in industrial applications, including as a filler material in plastics and papermaking.

ACKNOWLEDGEMENTS

The authors are very grateful to the Korea Institute of Energy Technology Evaluation and Planning through the ETI program, Ministry of Trade, Industry and Energy (Project No. 2013T100100021) for financial support of this research.

REFERENCES

1. P. Bernal and D. Oliva, The first global integrated marine assessment. World Ocean assessment 1. Chapter 12, United Nations, New York (2016).
2. FAO, The state of world fisheries and aquaculture, Food and Agriculture Organization of the United Nations (2014).
3. FAO, Global Aquaculture Production statistics database updated to 2013 Summary information, Food and Agriculture Organization of the United Nations (2015).
4. H. S. Kim, *The study of application of discarded oyster shell powder as an architectural material*, Master thesis, Korea (2007).
5. G. L. Yoon, B. T. Kim, B. O. Kim and S. H. Han, *Waste Manage.*, **23**, 825 (2003).
6. J. H. Jung, K. S. Yoo, H. G. Kim, H. K. Lee and B. H. Shon, *J. Ind. Eng. Chem.*, **13**, 512 (2007).
7. H. B. Kwon, C. W. Lee, B. S. Jun, J. D. Yun, S. Y. Weon and B. Koopman, *Resour. Conserv. Recy.*, **41**, 75 (2004).
8. S. Asaoka, T. Yamamoto, S. Kondo and S. Hayakawa, *Bioresour. Technol.*, **100**, 4127 (2009).
9. W. H. Park and C. Polprasert, *Ecol. Eng.*, **34**, 50 (2008).
10. N. Nakatani, H. Takamori, K. Takeda and H. Sakugawa, *Bioresour. Technol.*, **100**, 1510 (2009).
11. C. H. Lee, D. K. Lee, M. A. Ali and P. J. Kim, *Waste Manage.*, **28**, 2702 (2008).
12. H. B. Kwon, C. W. Lee, B. S. Jun, S. Y. Weon and B. Koopman, *Resour. Conserv. Recy.*, **41**, 75 (2004).
13. K. Mori and K. Takahashi, *Mizushorigijutu.*, **39**, 1 (1998).
14. R. A. F. de Alvarenga, B. M. Galindro, Cde. F. Helpa and S. R. Soares, *J. Environ. Manage.*, **106**, 102 (2012).
15. J. Hutchinson and A. D. O'Sullivan, *Scanning electron microscopy of substrates from bioengineered treatment reactors*, University of Canterbury, New Zealand (2008).
16. L. Xiang, Y. Xiang, Y. Wen and F. Wei, *Mater. Lett.*, **58**, 959 (2004).
17. Z. T. Yao, T. Chen, H. Y. Li, M. S. Xia, Y. Ye and H. Zheng, *J. Hazard. Mater.*, **262**, 212 (2013).
18. M. Suzuki, S. Sakuda and H. Nagasawa, *Biosci. Biotech. Bioch.*, **71**, 1735 (2007).
19. Z. T. Yao, M. S. Xia, H. Y. Li, T. Chen, Y. Ye and H. Zheng, *Crit. Rev. Env. Sci. Tec.*, **44**, 2502 (2014).
20. I. Corni, T. J. Harvey, J. A. Wharton, K. R. Stokes, F. C. Walsh and R. J. K. Wood, *Bioinspir. Biomim.*, **7**, 1 (2012).
21. M. H. Chong, B. C. Chun, Y. C. Chung and B. G. Cho, *J. Appl. Polym. Sci.*, **99**, 1583 (2006).
22. Z. D. Lin, Z. X. Guan, C. Chen and B. F. Xu, *Thermochim. Acta.*, **551**, 149 (2013).
23. E. Daniel and P. Luiz Antonio, *Mater. Res. Bull.*, **12**, 517 (2009).
24. H. Y. Li, Y. Q. Tan, L. Zhang, Y. X. Zhang, Y. H. Song, Y. Ye and M. S. Xia, *J. Hazard. Mater.*, **217**, 256 (2012).
25. P. M. A. de Melo, L. B. Silva, A. S. F. Santos, T. A. Passos, S. J. G. Lima and M. M. Ueki, Proceedings of 22nd International Congress of Mechanical Engineering, Ribeirao Preto (2013).
26. J. W. Ahn, W. K. Park, K. S. You, H. C. Cho, S. J. Ko and C. Han, *Solid State Phenom.*, **124**, 707 (2007).
27. W. K. Park, S. J. Ko, S. W. Lee, K. H. Cho, J. W. Ahn and C. Han, *J. Cryst. Growth*, **310**, 2593 (2008).
28. M. Holcomb, A. L. Cohen, R. I. Gabitov and J. L. Hutter, *Geochim. Cosmochim. Act.*, **73**, 4166 (2009).
29. C. Linga Raju, K. V. Narasimhulu, N. O. Gopal, J. L. Rao and B. C. V. Reddy, *J. Mole. Structure.*, **608**, 201 (2002).
30. J. Kuther, G. Nelles, R. Seshadri, M. Schaub, H. J. Butt and W. Tremel, *Chem. Eur. J.*, **4**, 1834 (1998).
31. Y. Ota, S. Inui, T. Iwashita, T. Kasuga and Y. Abe, *J. Am. Ceram. Soc.*, **78**, 1983 (1995).
32. L. F. Wang, I. Sondi and E. Matijevic, *J. Colloid Interface Sci.*, **218**, 545 (1999).
33. S. D. Skapin and I. Sondi, *J. Colloi Interface Sci.*, **347**, 221 (2010).
34. Z. S. Hu and Y. L. Deng, *J. Colloid Interface Sci.*, **266**, 359 (2003).
35. D. Rautaray, A. Banpurkar, S. R. Sainkar, A. V. Limaye, N. R. Pavaskar, S. B. Ogale and M. Sastry, *Adv. Mater.*, **15**, 1273 (2003).
36. G. Li, Z. Li and H. W. Ma, *Int. J. Min. Proc.*, **123**, 25 (2013).
37. C. Domingo, E. Loste, J. Gomez-Morales, J. Garcia-Carmona and J. Fraile, *J. Super, Flu.*, **36**, 202 (2006).